Evaluation of a Budget Optical Coherence Tomography for Cleaning Treatments of Painted Ancient Artifacts

Measurement Science
and Technology

PAPER • **OPEN ACCESS**

Evaluation of a budget optical coherence tomography for cleaning treatments of painted ancient artifacts

To cite this article: Chiara Bellezza Prinsi *et al* 2025 *Meas. Sci. Technol.* **36** 075206

OPEN ACCESS
IOP Publishing
Measurement Science and Technology
Meas. Sci. Technol. **36** (2025) 075206 (10pp)
https://doi.org/10.1088/1361-6501/ade89d

Evaluation of a budget optical coherence tomography for cleaning treatments of painted ancient artifacts

Chiara Bellezza Prinsi[1], Paola Buscaglia[2], Massimo Olivero[1,*], Alessandro Re[3], Sabrina Grassini[1], Alberto Vallan[1] and Guido Perrone[1]

[1] Politecnico di Torino, c.so Duca degli Abruzzi 24, 10129 Torino, Italy
[2] Fondazione Centro per la Conservazione ed il Restauro dei Beni Culturali (La Venaria Reale), Via XX Settembre 18, 10078 Venaria Reale, Italy
[3] Università di Torino and Istituto di Fisica Nucleare, via Pietro Giuria 1, 10125 Torino, Italy

E-mail: massimo.olivero@polito.it

Received 25 February 2025, revised 18 June 2025
Accepted for publication 26 June 2025
Published 15 July 2025

Abstract
This study investigates the accuracy of budget optical coherence tomography (OCT) for measuring the thickness of protective varnishes on ancient artifacts that have to undergo cleaning or restoration. Two sets of glass slides, deposited with layers that mimic the structure of ancient handcrafted objects (pigment and varnish), are analyzed. OCT measurements are compared with coating thickness gauge and destructive scanning electron microscope analysis. The results show that OCT provides reasonably accurate thickness measurements, with errors significantly lower than typical variability in cultural heritage applications. This suggests that even a low-cost OCT has the potential to become a valuable non-invasive tool for real-time monitoring of cleaning treatments of ancient artifacts.

Keywords: cultural heritage conservation, optical coherence tomography (OCT), thickness measurement, laser cleaning

1. Introduction

Cultural heritage conservation is an established discipline that has experienced continuous development since the nineteenth century, starting from empirical experience and onward evolving with scientific methodologies. In the last decades of the twentieth century, these have provided conservators with a number of tools to effectively investigate original artistic techniques and materials used. Nowadays, research is moving forward to the development of new efficient recovery and conservation methodologies.

Recent trends employ multi-analytical approaches [1] in which imaging techniques are used for an initial screening of the surface distribution of materials, followed by quantitative or semi-quantitative spot analysis for the chemical and morphological characterizations of micro-samples and/or for optical and electronic microscope investigations [2].

Among various analytical techniques for the characterization of materials, electron microscopy stands out for its ability to provide detailed information on the fine microstructure and stratigraphy of the surface. However, its routine and extensive use during conservation treatments is limited both because it is an invasive technique, i.e. small samples must be extracted from the artifact, and because the sample preparation for the

* Author to whom any correspondence should be addressed.

analysis is cumbersome and may influence the measurement outcomes. Other characterization techniques include multispectral imaging [3], possibly integrated with chemical analysis using Fourier transform infrared spectroscopy (FTIR) or gas chromatography-mass spectrometry. An accurate evaluation of the composition and thickness of at least the most superficial layer of an artifact provides essential information prior to any conservation treatment planning, in particular, when the treatment devises removal of substances from the original artifact. A typical example is the cleaning of painted surfaces, which is considered among the most challenging operations because of the potentially destructive impact.

The effectiveness and safety of a conservation procedure is commonly assessed by analyzing the surface before and after preliminary cleaning tests. However, this procedure may not be effective because the layers to be removed generally lack thickness homogeneity. Despite scientific research having provided many methods to guarantee gradual and selective removal of specific surface materials [4–6], it is difficult to objectively monitor the impact of any treatment in real time, going beyond subjective assessments by the conservator.

The scientific analysis carried out after an intervention provides details on the surface morphology, the presence of residues, and by sampling cross sections of the transition area of the cleaned surface, the variation in thickness. However, in the event of inadequate treatment, permanent damage occurs. For these reasons, the real challenge in monitoring cleaning treatments is having stratigraphic information with a non-destructive tool, which must also work in real time and be cost-effective [7], [8].

In addition to multispectral imaging, optics can provide other noninvasive techniques [9] to monitor cleaning treatments on painted surfaces, including colorimetric analysis [10], photoacoustics [11], profilometry [12], reflection infrared spectroscopy [13], and optical coherence tomography (OCT) [14].

In particular, OCT is attractive for its good balance between the information available and the complexity of use [15, 16]. OCT, exploiting either a low power broadband source or a swept laser, produces a cross-section image of semi-transparent samples, yielding fast sampling (images are produced within milliseconds) and micrometer resolution. In its simplest and low-cost implementation, OCT uses a low-coherence broadband light in the near infrared region (usually in the range 0.7–1.5 μm, with investigations at 2 μm using custom instruments [17]); this optical signal is reflected by the sample, which behaves as one arm of a Michelson interferometer. Interferometric patterns are collected and processed over a scanning length to return the internal structure of the sample. The result of the measurement is then shown as a map extending in depth to up to 3 mm and whose intensity levels depend on the refractive index and scattering coefficient of the materials. Because OCT is a non-contact technique and can be implemented as a portable instrument, it is commonly used in biomedical applications to obtain images of tissues below the surface [18], but it is proved to be a promising tool in the conservation of cultural heritage thanks to the development of new systems and segmentation algorithms [19]. However, studies published so far mainly report qualitative evaluations of the cleaning process evolution, without attempting to quantify the actual thickness of the layers, which instead requires an accurate estimation of their refractive index values [20]. Besides, OCT is very effective only when the layers under investigation are semitransparent and have a sufficient refractive index contrast. For these reasons, a recent work has highlighted that the most promising approach for effective aid during cleaning of artifacts is to combine OCT measurements with data from other techniques, such as FTIR spectroscopy [21]. Within this research, we are exploring a different approach, based on the combination of OCT measurements with fluorescence spectroscopy (FS), which may bring advantages in terms of equipment and measurement speed. FS allows rapid and reagent-free analysis of samples with little pre-processing and provides a 10–1000 fold higher sensitivity than other analytical techniques such as UV absorption measurements [22]. Moreover, many materials have characteristic fluorescence spectra, thus they can be used as natural fluorophores. This property can be exploited to detect specific chemical fingerprints and thus provide an additional tool to estimate the refractive index necessary to the OCT measurements by integrating FS measurements with machine learning techniques. As a preliminary step, it is necessary to separately validate the ability of the OCT to discriminate and measure the thickness of layers, in particular those of varnish and pigments, to be used as a portable aid during processes of cleaning and removal of layers of painted surfaces. In this first work, only the validation of the OCT alone is performed, but for the first time to the best of authors' knowledge, using a very simple commercial instrument [23] featuring acceptable characteristics at a price fourfold lower than the average, to prove that the OCT may enter the conservators' work bag. The primary objective is to assess whether such an instrument can provide reliable, reproducible, and non-invasive measurements suitable for both laboratory testing and potential *in situ* applications. Two sets of layered samples were prepared: the first, with well-defined and controlled layer thicknesses, was used to calibrate the measurement procedure; the second, featuring hand-applied layers that replicate typical coated painted surfaces, served as a testbed for OCT-based thickness evaluation. The OCT-derived measurements were validated through comparison with scanning electron microscopy (SEM), considered a benchmark technique for this type of analysis. Furthermore, a series of repeated OCT measurements was carried out to assess the reproducibility of the method. The subsequent sections are organized as follows: section 2 describes the sample preparation and experimental procedures, section 3 presents and discusses the results, including a real case study, and section 4 concludes the article with a summary and perspectives for future work.

2. Materials and methods

The potentiality of OCT for online monitoring of conservation treatments was investigated in a simplified, yet representative case of actual scenarios, where the thickness of a layer

of Paraloid® B72, a transparent protective material, must be quantified when it is deposited on Egyptian blue painting.

Paraloid® B72, an ethyl methacrylate-methyl acrylate copolymer, is one of the most used chemicals in the restoration of artifacts thanks to its properties of being stable, water-resistant and non-yellowing finish. It is extensively employed by conservators as a coating, consolidant, and adhesive, even if in some cases it leads to an increase in superficial gloss and in others to matting, yellowing, adhesion, and possible incorporation of atmospheric particulates. These alterations can compromise the accurate interpretation of original painting techniques and affect the outcome of scientific analysis, such as imaging and colorimetric measurements [24, 25].

Egyptian blue, a pigment used in Ancient Egypt, is a calcium copper silicate, whose accepted chemical formula is the same as cuprorivaite ($CaCuSi_4O_{10}$) [26]. It represents a relevant test-bench for optical techniques due to its high porosity and vivid coloration. Modern artworks or restored artifacts frequently exhibit irregular acrylic resin coatings over such pigments, making Egyptian blue a relevant model substrate.

2.1. Preparation of the samples

Two sets of samples were prepared by deposition of Paraloid® B72 and Egyptian blue layers glass microscope slides to replicate typical stratigraphies encountered in conservation. The layer structure of the two sets is illustrated in figure 1(a). The first set aimed at providing controlled conditions and would be used as a reference for calibration, while the second set was devised to validate the calibration process as in the nearly real case.

In the first set Paraloid® B72 was deposited using an industrial-grade professional sprayer onto both glass microscope slides and compressed tablets of Egyptian blue pigment. The sprayer was maintained perpendicular to the surface at a fixed distance of 20 cm, and coating thickness was verified with a coating thickness gauge. The resin solution was prepared at 20% v/v in acetone (70:30 acetone: Paraloid® B72). The subset of samples contained Paraloid® B72 on a glass slide and would be used to analyze the behavior of OCT in the case of a single material. To reduce porosity, Egyptian blue powder (Kremer pigment no. 10 060) was mechanically grounded and compressed into tablets without binders. For each substrate (glass and pigment), the deposition of Paraloid® B72 was repeated up to 5 times, creating a gradient of resin layer thicknesses.

The second set consisted of samples prepared by manual deposition to simulate real-world manual applications. Paraloid® B72 was mixed in acetone (20 vol% v/v) and then manually applied by repeated brushing to obtain samples with multiple layers of different thicknesses. Also, in this case, two subsets were prepared: the first having Paraloid® B72 directly deposited on the microscope slides, whereas the second having a background layer of Egyptian blue. For the preparation of the latter, Egyptian blue pigments in a water solution of Arabic gum (10% vol.) were manually applied on the microscope slides, producing a layer of about 1 mm. The brushing technique and the use of Arabic gum simulate traditional artistic practices. This second set was used to validate the calibration on samples with more realistic variability in surface morphology and resin distribution. The pigment layers in both sample sets were not standardized in thickness, as they were consistently thicker than the OCT penetration depth and thus did not interfere with the measurement of the varnish layers. No binder (e.g. Arabic gum) was added during the preparation of the compressed pigment tablets, since the pigment served solely as an inert substrate. As the calibration procedure targeted only the varnish layer, variations in pigment thickness or composition beneath it had no influence on the reliability of the results.

2.2. OCT

The experiments reported were performed with a Lumedica budget instrument [23] (figure 2(a)). The system exploits the spectral domain OCT scheme and is equipped with a broadband source at 840 nm, yielding an output power of just 750 μW, which can be considered non-perturbing even on light-sensitive materials such as those of ancient artifacts. The system has a depth resolution of 7 μm in air and a transverse resolution of 15 μm. The cross section of the sample under test is presented by the built-in software as a grayscale image with bright hues corresponding to high reflection/scattering sections.

Additional external processing based on artificial-intelligence-assisted segmentation can be applied to identify the various layers and associate a false-color map [27, 28]. The main parameters of the instrument were compared to about 15 OCTs, manufactured by brands that mainly operate in biomedical fields and some focusing on industrial applications. Considering those operating at around 800 nm, it turns out that the low-cost OCT used for this investigation is mainly limited by the lower scanning rate and lower sensitivity, whereas the resolution is similar to that of more costly instruments. Figure 2(b) provides a comparison of the main parameters between the budget OCT here employed and a reference instrument that is representative of the category of OCT operating at 800 nm [29]. While scanning rate is not an issue in the framework of cultural heritage conservation, since there is no need for dynamic acquisitions, a low sensitivity may reduce the capability of detecting different layers. The difference in sensitivity between the budget OCT and standard instrument, expressed as optical-signal-to-noise-ratio, is a non-negligible value of 6 dB. The challenge is to prove that budget OCT, worth a quarter of comparable instruments, can be used by a conservator as a useful aid in recognizing layers for accurate removal and subsequent restoration.

It should be recalled that OCT images exhibit a distorted representation of the actual cross section because the displayed thickness of each layer depends on its optical density, i.e. its refractive index n. If the measurement is through air ($n = 1$), the depth measurement corresponds to the actual depth, whereas it is magnified when the medium has $n > 1$. In order to measure the actual thickness of each layer, corrections must be applied [30]; these rely on a preliminary calibration performed on reference samples that exhibit layers of known

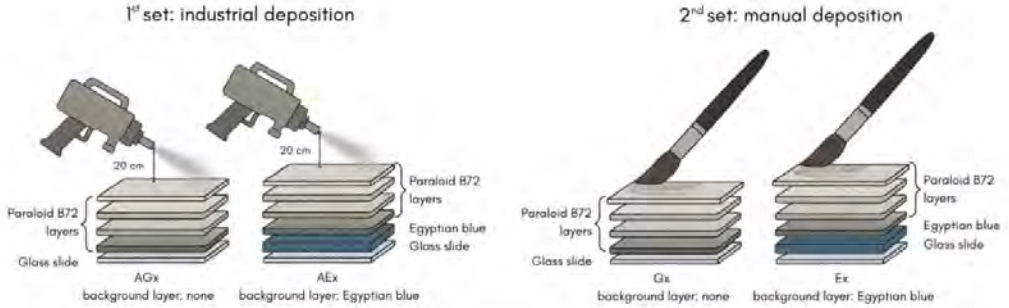

(a) Schematic of the fabrication process of the two sets of samples, performed by industrial deposition (1st set) and manual brushing (2nd set) respectively.

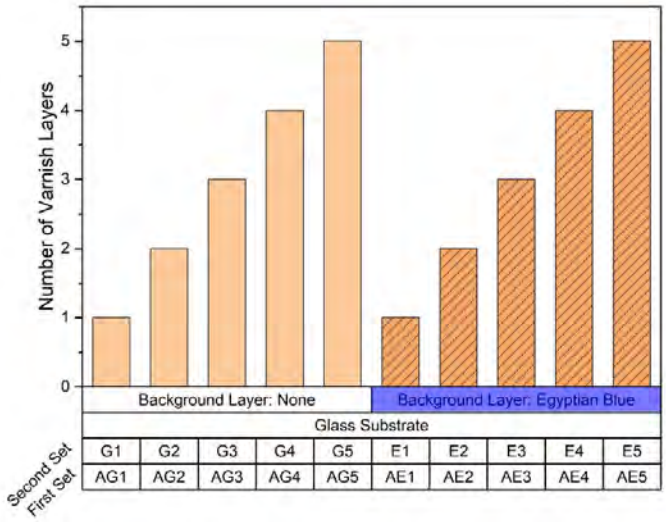

(b) Layer structure and corresponding coding of the samples. Samples designated as "AGx" refer to the 1st set, consisting of layers directly deposited on the glass slide, whereas "AEx" samples correspond to the 1st set deposited on an Egyptian blue substrate. On the other hand, codes "Gx" and "Ex" indicate the 2nd set, also deposited on glass and Egyptian blue substrates, respectively.

Figure 1. Samples fabrication and identification.

(a) Picture of the budget OCT used in this work (credit: Lumedica [23]).

Parameter	Budget OCT	Reference OCT
Central wavelength, nm	840	880
Sensitivity (OSNR), dB	100	106
Depth profile scan rate (A-scan), kHz	8.8	From 1.5 to 20
Depth resolution, µm	7	6
Price	~10k$	~40k$

(b) Comparison of main specs with a reference OCT [27]. Green-shaded cells highlight better values.

Figure 2. OCT system and specs. Reproduced with permission from Lumedica Labscope [23].

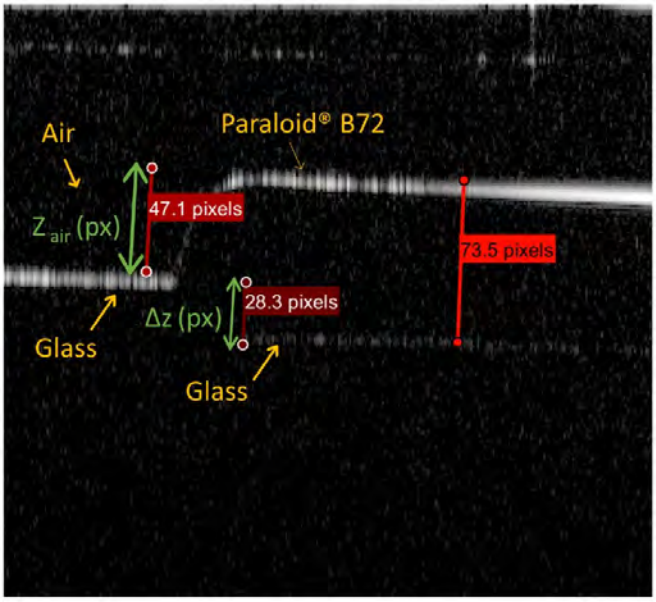

Figure 3. OCT image acquisition of sample G5 at the interface between glass and Paraloid® B72 layer. The image depicting the artifact of non-flat glass surface that is caused by the varnish, can be used to evaluate the refractive index of the deposited layer and to measure subsequent samples containing Paraloid® B72 layers.

material and thickness. The images from the Lumedica OCT have a resolution of 512 pixels for depth and each pixel corresponds to a different depth in μm according to the refractive index of the material. In the case of air, each pixel corresponds to 5.71 μm, meaning that the OCT has a maximum penetration of 2.92 mm in air. As an example, figure 3 depicts the OCT image of sample G5 at the edge of the Paraloid® B72 layer. It can be seen that the position of the glass surface moves downward on the right-hand side of the image, though the microscope slide is actually flat; this artifact is caused by the Paraloid® B72 layer that shifts the cross-sectional image due to its high refractive index. This highlights the importance of critical interpretation of OCT images in obtaining reliable information on thicknesses.

Defining Z_{air} as the optical thickness of the Paraloid® B72 layer in pixels measured in air, the conversion into the actual thickness T_{air} in μm is:

$$T_{\text{air}}\,(\mu\text{m}) = 5.71\,(\mu\text{m/px}) \cdot Z_{\text{air}}\,(\text{px}) \tag{1}$$

where 5.71 is the calibration factor.

Equation (1) is specific for the measurement of the thickness in air and can be generalized to T_{RI}, actual thickness for a generic refractive index (in equation (2)), measuring the optical thickness for a generic refractive index Z_{RI} (in pixels, equation (3)), taking into account Z_{air} and the difference Δz between the optical thickness in air and in another medium ($n > 1$) (more details are reported in [31]) .

$$T_{\text{RI}}\,(\mu\text{m}) = \frac{5.71\,(\mu\text{m/px}) \cdot (Z_{\text{air}} + \Delta z)\,(\text{px})}{n} \tag{2}$$

where

$$Z_{\text{air}} + \Delta z = Z_{\text{RI}} \tag{3}$$

Based on the information provided in figure 3 and applying equations (1) and (2), it turns out that for Paraloid® B72 $n \simeq 1.487$, in excellent agreement with the values reported in the literature [32, 33]. OCT is compared with coating thickness gauge and SEM to validate and calibrate the measurement procedure. Both methods, while being a reference for in-lab measurements and during sample preparation, do not permit monitoring 'on field'. In particular, the first requires the varnish to be measured during the deposition process, or at least while the varnish is still wet. On the other hand, SEM requires a micro-invasive sampling to allow the measurement of the layers thickness, giving a pre-treatment information, and is not considered suitable formonitoring during the intervention. In addition, SEM allows for a single measure in a limited number of locations to minimize damage, whereas OCT allows monitoring of the extended area and repeating the measurements multiple times during the cleaning intervention and throughout the aging process, thus ensuring a precise assessment of the effectiveness of the treatment and long-term stability.

3. Results and discussion

Each sample from the two sets was analyzed with OCT and then the recovered thickness values were compared with the reference thicknesses, either retrieved during the deposition or from SEM images, to validate the reliability of the OCT system during cleaning of artifacts. The OCT images were acquired and processed in MATLAB®, exploiting the image processing toolbox. Three images were taken for each sample to have a minimum amount of data to assess the accuracy of the measurement and uniformity of deposition. The outcome is reported in the categorical Tabs of figure 4, which reports the optical thickness in pixels as measured by the OCT as well as the correspondent thickness in μm. The thickness of the blue pigment in figure 4 is presented for illustrative purposes and is not to scale, as its exact thickness is not critical for the analysis. The focus of the study is on the measurement of the varnish layers, and the pigment thickness is significantly larger than the penetration depth of the OCT, meaning it does not impact the measurements in any way. In figure 4, the pigment layer thickness is shown only to provide clarity and improve the graph's readability, but it should not be considered as accurate or to scale. When comparing the two sets, a clear difference in deposition method emerges: the first subset, obtained using the industrial sprayer, shows a minimum layer thickness of approximately 20 μm, indicating a more controlled and uniform application. In contrast, the second

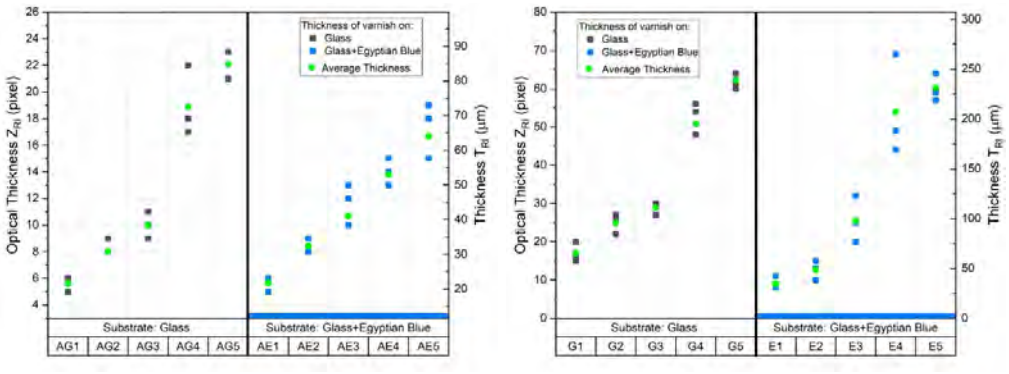

(a) First set: samples with layers deposited by an industrial sprayer

(b) Second set: samples prepared by manual brushing

Figure 4. Thickness measurement of first and second set of samples. The optical thickness of the varnish is reported in px on the left *y* scale, while the actual thickness in µm is displayed on the right *y* scale. Notice that the *x* axis reports the samples codes and their substrate structures NOT on scale.

subset, obtained via manual brushing, presents a thicker and more irregular layer, with an average thickness around 35 µm. However, in the case of direct deposition of Paraloid® B72 on glass the thickness has a non linear increment with the number of layers because the surface tension and poor adhesion produces a shrinkage of the varnish and hence a spurious assembling of material at the center of the glass, where the measure takes place. On the other hand, samples AE1–AE5 deposited on Egyptian blue show better adhesion and improved uniformity, as demonstrated by the nearly linear increment of thickness as a function of the number of layers. This does not hold for the second set, even for samples E1–E5 where the adhesion to the hand-brushed Egyptian blue is lower. Both deposition processes of Paraloid® B72 were performed using a 'wet-on-dry' technique, where the first layer of Paraloid® B72 was allowed to dry before the next layer was applied.

The OCT measurements for the first set of samples were compared to those from the coating thickness gauge (Erichsen, Wet Film Thickness Gauge Model 333, Measuring range 0–120 µm, Read-off accuracy 5 µm). Figure 5 shows the OCT image of sample AE3, containing both the Egyptian blue layer and three Paraloid® B72 layers. The varnish is well detectable, whereas the interface with the glass substrate is masked by the absorbing Egyptian blue.

The comparison between the OCT and coating thickness gauge measurements is summarized in figure 6 and shows that a maximum deviation of 12 µm occurs on the samples with Paraloid® B72 only because it is susceptible to shrinkage and produces areas of non-uniform varnish distribution. This effect is also observable on AE1–AE5 samples that have the varnish deposited on the industrial-made painting that also enhances the surface tension effect. The results are satisfactory, considering the lack of information on the uncertainty of the coating thickness gauge, which only provides the nominal value. In addition, concerning the deviation within values of 30 µm emerged in the thicker layers (G5 and E5), the potentially incomplete film formation of the Paraloid® B72 layer likely contributed to its thickness reduction from compression during the glass slide cutting process.

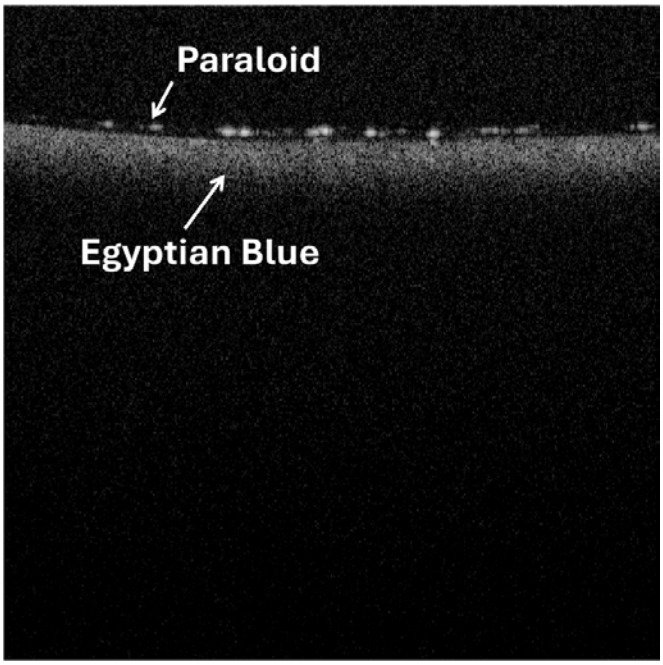

Figure 5. Example of OCT image of the sample AE3.

3.1. Validation of the reliability of the OCT measurements of handcrafted samples

The ability of the OCT to work in a realistic scenario of artifacts cleaning was assessed by comparing the OCT measurements of the second set of samples, i.e. fabricated by manual deposition of pigment and varnish, with those obtained by SEM (Zeiss Supra40 Field Emission SEM), which would be used as a reference. After acquisition of OCT images,

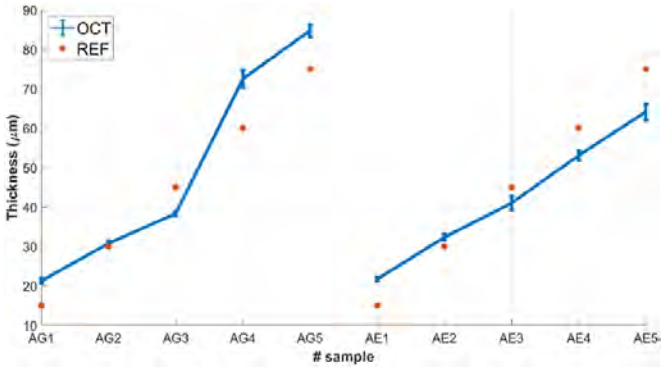

Figure 6. Comparison of the thickness of the Paraloid® B72 layer measured by OCT with the reference (coating thickness gauge) for the first set of samples (deposited by an industrial sprayer).

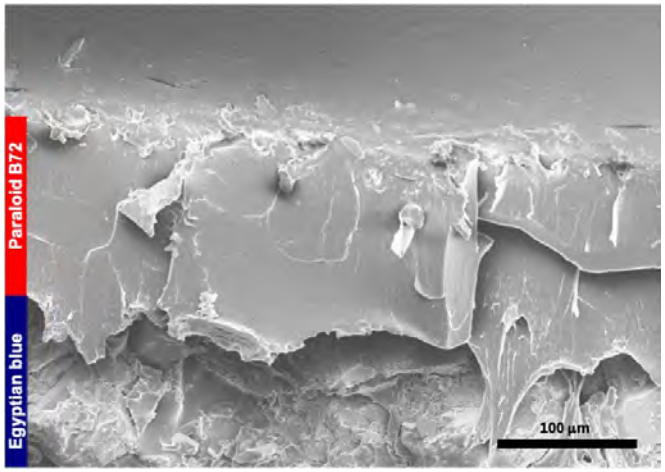

Figure 7. SEM image of the cross-section of sample E5 with the detail of the Paraloid® B72 layer. From top: Paraloid® B72 and Egyptian blue layers on the glass substrate (not visible in the picture). The Paraloid® B72 layer thickness is estimated to be 203.4 μm.

each sample was sharp cut at 1 cm from the edge, paying attention to preserve the cross section. The cut-off interface was coated with an electrically-conducting platinum thin film (about 10 nm), to enhance the contrast while preserving the layer pattern. As an example, figure 7 reports a cross-section image of the E5 sample. The interface between the Paraloid® B72 and the Egyptian blue layers is observable as the varnish appears more compact and smooth than the pigment.

Figure 8 shows the correspondent OCT image (figure 8(d)) along with those of samples G1, E1 and G5. In the case of samples G1 and G5, the flatness of the background surface of the supporting glass results in a more uniform thickness. Figure 9 also highlights, for given a number of varnish layers, samples with the Egyptian Blu substrate exhibit a lower thickness of Paraloid® B72 compared to those with glass substrate. This difference is ascribed to the porosity of the pigment layer, which leads to absorption of the varnish into the pigment layer. Such an effect is better observable in figure 8(c), where the Paraloid® B72 partially gets blurred within the Egyptian blue substrate, while in figure 8(d) the Paraloid® B72 is does not outdiffuse in the glass substrate. It is important to note that no significant swelling (i.e. macroscopic volume expansion) of the varnish layer was observed; the reduction in apparent thickness is solely due to the absorption of Paraloid® B72 into the pores of the pigment. Evidence of the porosity of Egyptian blue can also be assessed by comparing figures 8(d) and 5, wherein the latter the pigment layer (i.e. the lower one) is more compact than the corresponding one in the first image.

The porosity of the material can be a problem during the usage of the OCT in a real framework, since the detection of thin varnish layers in porous materials can be tricky to distinguish for untrained users, though a keen eyesight analysis may detect the presence of the varnish as a higher concentration of bright spots on top of pigment layer, as in the case shown in figure 8(c).

Figure 9 compares the thickness measurements from OCT and from SEM. Due to limited access to the latter, the comparison could be performed on a few samples.

The OCT measures exhibit a larger error bar than those measured from SEM images, in particular for the samples containing Egyptian blue pigment. This is because the Egyptian blue absorbs the varnish making it difficult to discriminate accurately between the pigment and the upper layer.

The thickness values obtained through OCT imaging were compared to reference data acquired via SEM and coating thickness gauges. The absolute error ranged from 0.5 μm to 30.2 μm (for a thickness value of about 230 μm), depending on layer homogeneity and thickness. A Pearson correlation analysis revealed a statistically significant correlation ($r = 0.991$), supporting the accuracy of the low-cost OCT device in measuring the layers of transparent varnish. It should be noted that our comparison has an inherent source of error in the preparation of the samples for SEM analysis because a random compression of the layers can occur during the cutting, as significantly recognizable in sample G5. Further investigations shall overcome this issue by implementing advanced dicing techniques, such as femtosecond laser cross-sectioning, as proposed by Harada *et al* [34]. Overall, the comparison still supports the use of the budget OCT on artifacts and cultural heritage handcrafts, possibly increasing the accuracy by complementing it with fluorescence analysis. Yet, non-contact in-situ measurements performed without sample preparation make a point of using OCT in art conservation.

3.2. Reproducibility of the sample

The reproducibility of the sample was evaluated by taking 50 repeated measurements on samples G4 and E4. The measurements were taken at 10 different locations in each sample, acquiring 5 images for each spot. As summarized in figure 10, there is better agreement among measures on sample E4, where the phenomenon of shrinking of the varnish is attenuated by the enhanced adhesion of to the pigment layer. On the other hand, sample G4 exhibits a larger variability due to the inhomogeneity of the Paraloid® B72 film across the glass substrate. However, it is important to point out that, for each acquisition, the spread of the measurements is well within

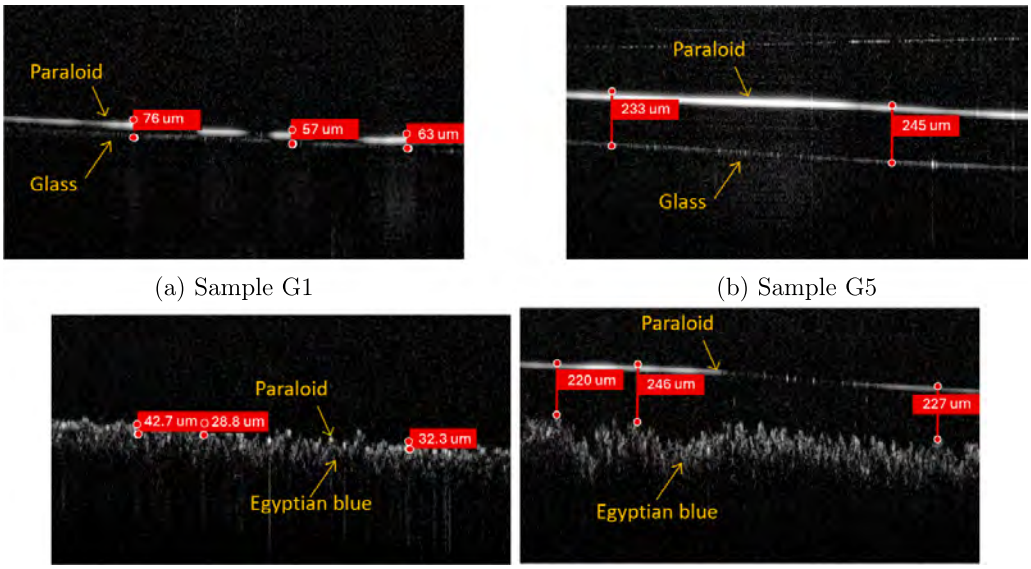

(a) Sample G1 (b) Sample G5

(c) Sample E1 (d) Sample E5

Figure 8. OCT images of the second set (samples produced by manual deposition of Egyptian Blue and Paraloid® B72 layers.).

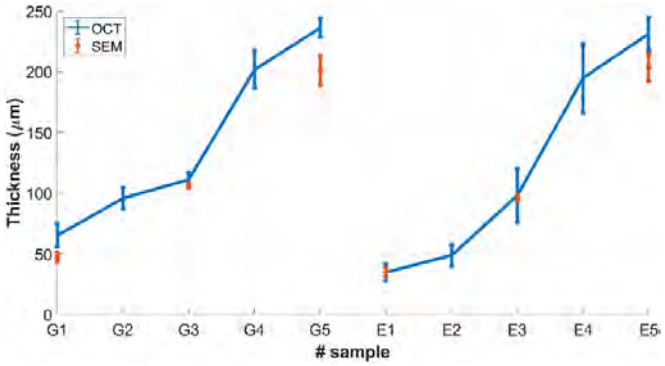

Figure 9. Comparison of the thickness of the Paraloid® B72 layer measured by OCT and SEM for the second set of samples.

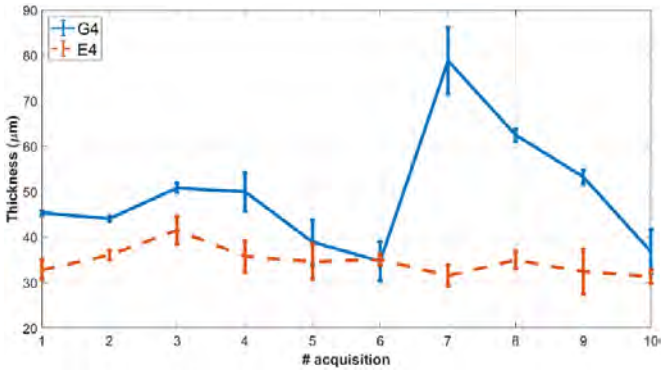

Figure 10. Mean and standard deviation of Paraloid® B72 thickness on samples G4 and E4.

acceptable ranges for the intended application. This means that the thickness of the Paraloid® B72 layer can be measured with enough accuracy within the small acquisition area of the OCT (7 mm).

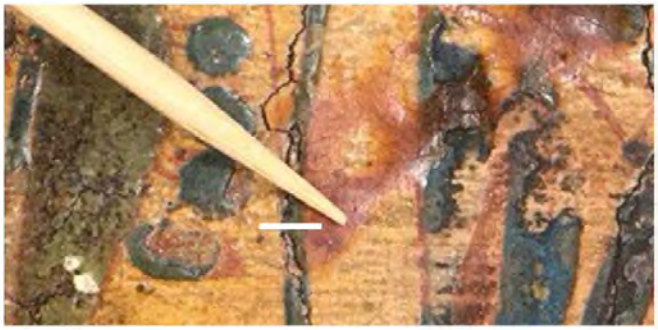

Figure 11. Egyptian artifact. The white line indicates the cross section of OCT measurements.

3.3. Case study on an Egyptian artifact

Since the measurements on prepared samples yielded satisfactory results, the OCT was tested on an ancient Egyptian wooden coffin, applying the calibration described in previous sections. Figure 11 reports a picture of the analyzed area, where the artifact white line indicates the location of the OCT measurement. At that position, the artifact has a dark painted line partially covered by ancient mastic, whereas the area is coated by a Paraloid® B72 layer that was deposited during a previous intervention.

Figure 12 shows the correspondent OCT image.

The layer thickness was evaluated by applying the procedure described in section 2.2. In all the points measured, a value of 15.4 μm was obtained, with deviations between 0.9 μm and 4.8 μm, thus suggesting a discrete overestimation of OCT measurements. Concerning the point of analysis of figure 11, of a value of 31.7 μm, a higher variability of the Paraloid® B72 layer might be hypothesized and ascribed to the hand-made deposition of the varnish during the previous intervention. The system's ability to acquire over 100 *b*-scans within a 1 × 7 mm

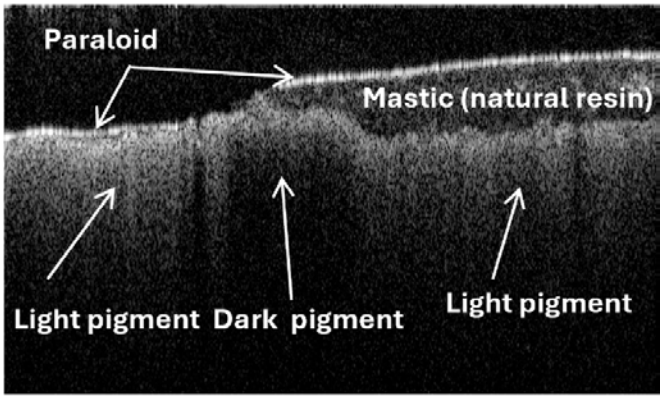

Figure 12. OCT image correspondent to the white line of figure 11. The Paraloid® B72 layer thickness is estimated to be 31.7 µm.

analysis area underscores its potential for comprehensive, non-destructive mapping of layer thickness variability, offering a promising approach for detailed material distribution on the surface.

4. Conclusions

The paper has presented the use of a low-cost OCT instrument, to evaluate the thickness of transparent varnish (in particular Paraloid® B72) that is often found as a protective layer on ancient paints and artifacts, which has to be removed with a view to conservation treatments. The assessment has been carried out on two different sets of samples, consisting of microscope slides coated with pigment and varnish. The first set, where the deposition was made with a professional varnishing setup, has been used as reference for the calibration of the procedure, while the second set, made by hand brushing the varnish to mimic real artifacts, has been used as a testbed for thickness evaluation through OCT. The thicknesses estimated from OCT images resulted in good agreement with the measurements from SEM images, which is considered a reference technique for the characterization of artifacts. A campaign of repeated measurements has been carried out to evaluate the reproducibility of the OCT measurements, resulting in well below the usual thickness variability of artifacts, hence demonstrating the potentiality of the approach to consistently measure the thickness of the Paraloid® B72 layer. Finally, the estimation of the Paraloid® B72 thickness on an ancient Egyptian coffin has been performed, reporting a slight overestimation with respect to microscope analysis, performed on micro-samples, due to inherent measurement limitations: the pixel-to-micron conversion factor imposes a quantization constraint, equal to a minimum of 5.71 µm (equivalent to one pixel). Interestingly, the accuracy of the thickness quantification can be assumed also for different resins, calibrating the values with the specific refractive index, as highlighted in the activity performed in the case study, even if the overall results should be considered preliminary because the experimental investigation should be extended to different varnishes and to an evaluation of the change of the refractive index linked to the aging of the materials. Moreover, the OCT measurements shall be complemented with other non-destructive techniques that are capable of providing chemical/physical information of the materials, such as the FS we are exploring. Yet, this research demonstrates that a budget OCT can be used as a handheld and real-time monitoring tool for varnish removal.

Data availability statement

All data that support the findings of this study are included within the article (and any supplementary files).

Acknowledgments

The authors acknowledge Dr Enrico Ferraris (Museo Egizio di Torino, Italy) and Dr Matilde Borla (Soprintendenza Archeologia, Belle Arti e Paesaggio per la Città Metropolitana di Torino, Italy), for permission to perform additional measurements on the case study. Furthermore, acknowledgments are due to Scientific Laboratories of Centro Conservazione Restauro 'La Venaria Reale', for SEM analysis. This work was partially carried out at PhotoNext Inter-Department Center of Politecnico di Torino.

References

[1] Duivenvoorden J R *et al* 2025 How to approach long-term monitoring of chemical dynamics in oil paintings? *npj Herit. Sci.* **13** 24
[2] Fontana R, Bellini M, Corsi C, Mastroianni M, Materazzi M, Pezzati L and Tortora A 2007 Optical coherence diagnostics for painting conservation *Proc. SPIE* **6618** 661808
[3] Es Sebar L, Lombardo L, Buscaglia P, Cavaleri T, Lo Giudice A, Re A, Borla M, Aicardi S and Grassini S 2023 3D multispectral imaging for cultural heritage preservation: the case study of a wooden sculpture of the Museo Egizio di Torino *Heritage* **6** 2783–95
[4] Husby L M, Andersen C K, Pedersen N B and Ormsby B 2023 Evaluating three water-based systems and one organic solvent for the removal of dammar varnish from artificially aged oil paint samples *Herit. Sci.* **11** 244
[5] Biribicchi C, Giuliani L, Macchia A and Favero G 2023 Organogels for low-polar organic solvents: potential applications on cultural heritage materials *Sustainability* **2023** 16305
[6] Manfredda N *et al* 2021 An ancient Egyptian multilayered polychrome wooden sculpture belonging to the museo Egizio of Torino: characterization of painting materials and design of cleaning processes by means of highly retentive hydrogels *Coatings* **11** 1335
[7] Catelli E *et al* 2022 Towards the non-destructive analysis of multilayered samples: a novel XRF-VNIR-SWIR hyperspectral imaging system combined with multiblock data processing *Anal. Chim. Acta* **1239** 340710
[8] Volino A, Lumaga M R B, Cennamo P, Fatigati G and Trojsi G 2018 Multidisciplinary approach for the study of the Ptolemaic coffin of Ankhhapy from the Egyptian collection of MANN in Naples *2018 Metrology for Archaeology and Cultural Heritage (MetroArchaeo)* pp 6–11
[9] Thickett D, Cheung C S, Liang H, Twydle J, Maev R G and Gavrilov D 2017 Using non-invasive non-destructive

techniques to monitor cultural heritage objects *Insight, Non-Destr. Test. Cond. Monit.* **59** 230–4
[10] Angelini E, Grassini S, Piantanida M, Corbellini S, Ferraris F, Neri A and Parvis M 2010 FFT-based imaging processing for cultural heritage monitoring *2010 IEEE Instrumentation & Measurement Technology Conf. Proc.* pp 1106–11
[11] Dimitroulaki E, Tserevelakis G J, Melessanaki K, Zacharakis G and Pouli P 2023 Photoacoustic real-time monitoring of UV laser ablation of aged varnish coatings on heritage objects *J. Cult. Herit.* **63** 230–9
[12] Sansoni G and Docchio F 2005 3-D Optical Measurements in the Field of Cultural Heritage: the Case of the Vittoria Alata of Brescia *IEEE Trans. Instrum. Meas.* **54** 359–68
[13] Corbellini S, Ferraris F, Neri A, Parvis M, Angelini E and Grassini S 2011 Exposure-tolerant imaging solution for cultural heritage monitoring *IEEE Trans. Instrum. Meas.* **60** 1691–8
[14] Targowski P, Iwanicka M, Tymińska-Widmer L, Sylwestrzak M and Kwiatkowska E A 2010 Structural examination of easel paintings with optical coherence tomography *Acc. Chem. Res.* **43** 826–36
[15] Striova J, Salvadori B, Fontana R, Sansonetti A, Barucci M, Pampaloni E, Marconi E, Pezzati L and Colombini M P 2015 Optical and spectroscopic tools for evaluating Er:YAG laser removal of shellac varnish *Stud. Conserv.* **60** S91–S96
[16] Antoniuk P, Strakowski M, Pluciński J and Kosmowski B 2012 Non-Destructive Inspection of Anti-corrosion protective coatings using optical coherent tomography *Metrol. Meas. Syst.* **19** 365–72
[17] Read M, Cheung C S, Liang H, Meek A and Korenberg C 2022 A non-invasive investigation of Egyptian faience using long wavelength optical coherence tomography (OCT) at 2 μm *Stud. Conserv.* **67** 168–75
[18] Saikia M J 2021 A spectroscopic diffuse optical tomography system for the continuous 3-D functional imaging of tissue—a phantom study *IEEE Trans. Instrum. Meas.* **70** 1–8
[19] Monemian M and Rabbani H 2021 Analysis of a novel segmentation algorithm for optical coherence tomography images based on pixels intensity correlations *IEEE Trans. Instrum. Meas.* **70** 1–12
[20] Iwanicka M, Kwiatkowska E, Sylwestrzak M and Targowski P 2011 Application of optical coherence tomography (OCT) for real time monitoring of consolidation of the paint layer in Hinterglasmalerei objects *Proc. SPIE* **8084** 80840G
[21] Iwanicka M, Moretti P, van Oudheusden S, Sylwestrzak M, Cartechini L, van den Berg K J, Targowski P and Miliani C 2018 Complementary use of optical coherence tomography (OCT) and reflection FTIR spectroscopy for *in-situ* non-invasive monitoring of varnish removal from easel paintings *Microchem. J.* **138** 7–18
[22] Bridgeman J, Baker A, Brown D and Boxall J 2015 Portable LED fluorescence instrumentation for the rapid assessment of potable water quality *Sci. Total Environ.* **524** 338–46
[23] AAVV 2023 Lumedica Labscope (available at: www.lumedicasystems.com/oq-labscope/) (Accessed 7 December 2023)
[24] Koob S P 1986 The use of Paraloid B-72 as an adhesive: its application for archaeological ceramics and other materials *Stud. Conserv.* **31** 7–14
[25] Horie V 2013 *Materials for Conservation: Organic Consolidants* (*Adhesives and Coatings*) 2nd edn pp 1–489
[26] Tite M, Bimson M and Cowell M 1984 *Technological Examination of Egyptian Blue* (ACS Pubrications) ch 11, pp 215–42
[27] Maloca P M *et al* 2019 Validation of automated artificial intelligence segmentation of optical coherence tomography images *PLoS One* **14** 1–14
[28] Drass M, Berthold H, Kraus M A and Müller-Braun S 2021 Semantic segmentation with deep learning: detection of cracks at the cut edge of glass *Glass Struct. Eng.* **6** 21–37
[29] Thorlabs 2025 GAN111C1/M spectral domain OCT system (available at: www.thorlabs.com/thorproduct.cfm?partnumber=GAN111C1/M) (Accessed 17 February 2025)
[30] Madruga F, Sfarra S and Real E 2020 Complementary use of active infrared thermography and optical coherent tomography in non-destructive testing inspection of ancient marquetries *J. Nondestruct. Eval.* **39** 1–8
[31] Bellezza C, Buscaglia P, Olivero M, Grassini S, Vallan A and Perrone G 2024 *2024 IEEE Int. Instrumentation and Measurement Technology Conf. (I2MTC)* pp 1–6 (available at: https://api.semanticscholar.org/CorpusID:270798231)
[32] 2024 Paraloid b72 refractive index (available at: https://cameo.mfa.org/wiki/Paraloid_B-72) (Accessed 31 July 2024)
[33] 2024 Paraloid b72 refractive index (available at: https://cool.culturalheritage.org/jaic/articles/jaic42-02-011.html) (Accessed 31 July 2024)
[34] Harada T, Spence S, Margiolakis A, Deckoff-Jones S, Ploeger R, Shugar A N, Hamm J F, Dani K M and Dani A R 2017 Obtaining cross-sections of paint layers in cultural artifacts using femtosecond pulsed lasers *Materials* **10** 107